Standing spin waves excited optically across an indirect gap in short graphene nanoribbons

Jun-Qiang Lu,[1] X.-G. Zhang,[1,2] and Sokrates T. Pantelides[3,4]
[1]*Center for Nanophase Materials Sciences, Oak Ridge National Laboratory, Oak Ridge, Tennessee 37831, USA*
[2]*Computer Science and Mathematics Division, Oak Ridge National Laboratory, Oak Ridge, Tennessee 37831, USA*
[3]*Materials Science and Technology Division, Oak Ridge National Laboratory, Oak Ridge, Tennessee 37831, USA*
[4]*Department of Physics and Astronomy, Vanderbilt University, Nashville, Tennessee 37235, USA*
(Received 12 January 2009; published 20 February 2009)

We report theoretical investigations that unveil unique electronic excitations in graphene nanoribbons of *nanoscale length*. The main point is that electronic states in short nanowires are standing particle-in-a-box-like waves, amenable to excitation by electromagnetic radiation. The unusual electronic and magnetic properties of graphene nanoribbons add another feature: terahertz (THz) radiation induces *edge standing spin waves* with different wavelengths at the two edges and a resonant frequency that can be controlled by an external gate voltage, opening the possibility of THz-spintronic applications.

DOI: 10.1103/PhysRevB.79.073408 PACS number(s): 73.21.Hb, 73.50.Mx, 73.63.Nm

Graphene has attracted considerable attention because of its unique electronic structure and properties. It was recently found that graphene ribbons of *nanoscale width*, known as nanoribbons,[1–3] have a small energy gap formed by edge states with opposite spin polarization. The gap can be tuned by an external gate field.[4] The energy gap, however, is indirect, which is unsuitable for optical excitations.

According to the Bloch theorem, electronic states in infinite periodic systems are *propagating waves* with wave vector $\mathbf{k}$. Excitations by electromagnetic (EM) radiation can only be "direct transitions" with $\Delta\mathbf{k}=0$. Thus, materials with indirect energy gaps, e.g., Si, are not suitable for optical applications. In a finite fragment of a periodic system, electronic states are in principle *standing waves* made up of $\pm\mathbf{k}$ Bloch states of the infinite system with $\mathbf{k}$ vectors restricted by the boundary conditions as in the simple case of a "particle in a box." This fact has negligible consequences in a macroscopic finite system except near the surfaces. In a metal, the surfaces induce Friedel oscillations that extend a few nanometers into the solid and decay like a polynomial.[5] Thus, to an excellent approximation, the bulk of a finite macroscopic sample behaves like an infinite solid. Surface-induced Friedel oscillations, however, have been recognized to play significant roles in nanostructures, notably in transport properties.[6] Here we focus on the fact that, for a nanoscale-length crystalline fragment, the effects of the opposite surfaces act synergistically and can give rise to a set of electronic states with unique optical-excitation modes, especially in the case of indirect energy gaps. One might say that different kinds of energy bands in the underlying material can produce unique particle-in-a-box optical-excitation features.

We shall demonstrate the phenomenon by explicit calculations in the case of zigzag graphene nanoribbons (ZGNR) (Refs. 1–3) of nanoscale width and nanoscale length (Fig. 1). The unique electronic structure of ZGNRs imparts additional features to the phenomenon as follows. In infinite ZGNRs, the energy gap is indirect and is defined by "edge states[7]" (analogs of surface states of three-dimensional systems) that exhibit ferromagnetic ordering in opposite directions.[4,8] Electromagnetic radiation cannot induce transitions across the indirect gap. For a nanoribbon of nanoscale length, however, the indirect gap becomes an asset, generating unique particle-in-a-box-like electronic states that are amenable to optical excitation. The optically excited standing waves of interest here are "edge standing spin-density waves," whose wavelengths are determined by the wave vectors of the valence-band and conduction-band extrema as we shall explain later. Noncollinear excitations are negligible due to very high spin-wave stiffness.[9] Furthermore, it is known that the ZNGR energy gap between occupied and empty edge states is tunable by a transverse dc electric field: the gap of one spin increases while the gap of the other spin decreases with the system becoming half metallic at some field value.[4] As a result, one can tune the driving photon frequency that sets up the standing spin waves. The resonant frequencies, corresponding to the energy gap, span the THz range. Thus, experimental detection of the effect can provide detailed information of the energy bands as a function of the transverse electric field. In addition, the pertinent photon frequencies can be tuned from zero to the THz region of the electromagnetic spectrum where the design of devices has been challenging because of the lack of materials with suitable response.[10] Thus, graphene nanoribbons (GNR) open the possibility for nanoscale "THz-spintronic" applications.

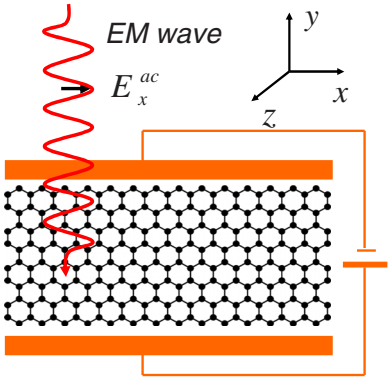

FIG. 1. (Color online) A zigzag graphene nanoribbon in x-y plane with a transverse dc electric field along the y direction and an electromagnetic wave incident along the z direction (perpendicular to the paper).

We turn now to an explicit calculation of the effect in ZGNRs. We note that first-principles calculations of the optical spectra of thin but infinite armchair GNRs were reported recently.[11] It was found that excitonic effects are large. Such calculations would be prohibitive for nanoscale-length GNRs. Instead, in order to demonstrate the effect of interest here, we adopt the following model Hamiltonian that includes only the carbon p_z orbitals perpendicular to the GNR plane but reproduces accurately the band structure of an infinite ZGNR near the Fermi energy:

$$H = \sum_{i\sigma} E_{i\sigma} c_{i\sigma}^{\dagger} c_{i\sigma} + \sum_{ij\sigma} t_{ij} c_{i\sigma}^{\dagger} c_{j\sigma}, \tag{1}$$

where $c_{j\sigma}(c_{j\sigma}^{\dagger})$ annihilates (creates) an electron with spin σ at atom site j of ZGNR, and $\sigma=\alpha,\beta$ (spin up and down). The spin-polarized onsite energies contain contributions from the mean-field magnetic (J_{ij}) and Coulomb (U_{ij}) interactions,

$$E_{i\sigma} = \pm \sum_{i\neq j} J_{ij} m_j + \sum_{ij} U_{ij} n_j, \tag{2}$$

where + is taken for $\sigma=\alpha$ and − is taken for $\sigma=\beta$; $m_j = \langle c_{j\alpha}^{\dagger} c_{j\alpha} - c_{j\beta}^{\dagger} c_{j\beta} \rangle$ and $n_j = \langle c_{j\alpha}^{\dagger} c_{j\alpha} + c_{j\beta}^{\dagger} c_{j\beta} \rangle$ are the local magnetization and local "charge" at site j, respectively. The hopping terms are $t_{ij}=t$ if i and j are nearest neighbors, and $t_{ij}=t'$ if i and j are second-nearest neighbors. The t' term breaks the electron-hole symmetry[12] and is necessary to reproduce the indirect band gap in the spin-resolved electronic structure. For the magnetic coupling we take $J_{ij}=J$ if i and j are nearest neighbors; $J_{ij}=0$ otherwise. The Coulomb term is necessary for reproducing correctly the change in the spin-dependent band gap as a function of the transverse electric field predicted by first-principles calculations.[4] This term includes two effects: the direct Coulomb interaction between the p_z electrons and the screening effect due to valence electrons not included in this model. Therefore we use the form $U_{ij}=1/(\epsilon r_{ij})$, where r_{ij} is the distance between sites i and j. The effective dielectric constant ϵ accounts for the screening effects from the valence electrons. The onsite Coulomb energy, $U_{ii}=U_0$, is treated as an additional parameter. The edge dangling bonds do not enter the Hamiltonian. In Ref. 4 they are saturated by hydrogen. Other mechanisms such as edge reconstruction may also passivate the dangling bonds but such a reconstruction merely moves the dangling-bond energy levels away from the Fermi energy and does not affect the bands relevant to Eq. (1).[13]

The parameters used in the calculations are: $t=-2.7$ eV, $t'=0.2t=-0.54$ eV,[12] $J=0.9$ eV, $U_0=6.08$ eV, and $\epsilon=3.68$. The lattice constant of graphene is $a=0.246$ nm. We used a ZGNR with eight chains (eight-ZGNR), which is the smallest width considered in Ref. 4. Figure 2(a) shows the band structure of the eight-ZGNR without a transverse dc electric field. The bands for the two spins are degenerate with a band gap of 0.3 eV. Figure 2(b) shows the band structure of the eight-ZGNR under a transverse dc electric field $E_y^{\mathrm{dc}}=2.0$ V/nm. The inset shows that the top of the valence band reaches the bottom of the conduction band, closing the indirect band gap (the bottom of the conduction band is located at $k_c=\pi/a$ and the top of the valence band at $k_v \approx 0.8\pi/a$). In Fig. 2(c) we show the change in the spin-dependent band gap as a function of the electric field. These results demonstrate that the semiempirical Hamiltonian defined above reproduces corresponding first-principles results with sufficient accuracy.[4]

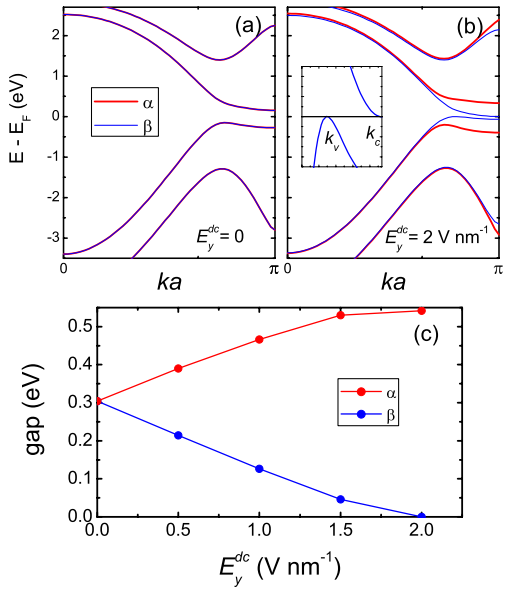

FIG. 2. (Color online) Spin-resolved band structure of an eight-ZGNR (a) with $E_y^{\mathrm{dc}}=0$ and (b) $E_y^{\mathrm{dc}}=2$ V/nm closes the band gap; (c) Change in the spin-resolved band gap of the eight-ZGNR as a function of E_y^{dc}.

Next we use Eq. (1) to examine the electronic structure of an 8-ZGNR fragment with a finite length, containing 99 carbon atomic lines (49.5 atomic units) in the x direction. We refer to this structure as (8,99) ZGNR. The highest occupied molecular orbital (HOMO)-lowest unoccupied molecular orbital (LUMO) gap of the (8,99) ZGNR vanishes at a transverse dc electric field $E_y^{\mathrm{dc}}=1.752$ V/nm. The wave functions of the HOMO and the LUMO in both spins are standing waves localized along the edges of the ZGNR. At zero external field, the HOMO and LUMO have periods given by $2\pi/k_v$ and $2\pi/k_c$, respectively (here k_v and k_c are the allowed wave vectors nearest the infinite-ribbon k_v and k_c, respectively). Each wave function is distributed symmetrically on the two edges. When an electric field is present, a remarkable feature appears in the wave functions, illustrated in Fig. 3 for an external dc field $E_y^{\mathrm{dc}}=1.745$ V/nm. The HOMO localizes more on the "top" edge with a period that is still $2\pi/k_v$ on both edges (k_v changes slightly as a function of the external field); the LUMO, on the other hand, retains the period $2\pi/k_c$ on the "bottom" edge where it is preferentially localized but acquires a period of $2\pi/k_v$ on the other edge. We will see later that these periods determine the periods of the charge and spin waves set up by pertinent external radiation.

We now turn to the response of the (8,99) ZGNR under an external ac EM field. We first study the low-frequency (GHz) response away from resonances and focus on the formation of the edge standing spin waves. The resonance in the THz range will be discussed later. In addition to the transverse dc field $E_y^{\mathrm{dc}}=1.745$ V/nm, we add an ac electric field with a frequency $\omega=16$ GHz ($\hbar\omega=0.01$ meV) and a small ampli-

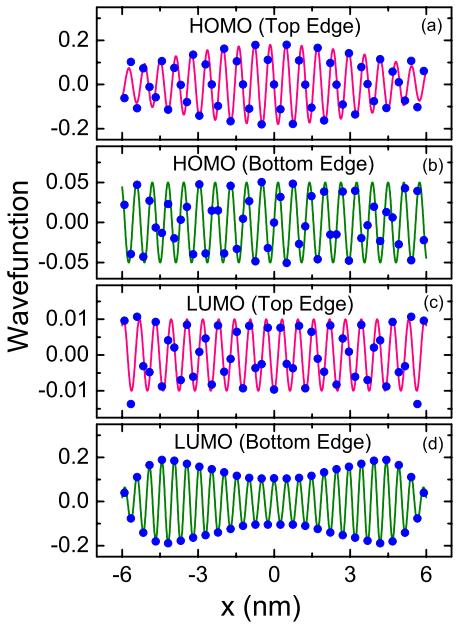

FIG. 3. (Color online) The wave function of HOMO/LUMO at [(a) and (c)] the top edge and [(b) and (d)] the bottom edge of the (8,99) ZGNR. The curves added in (a)–(d) are guides for the eye.

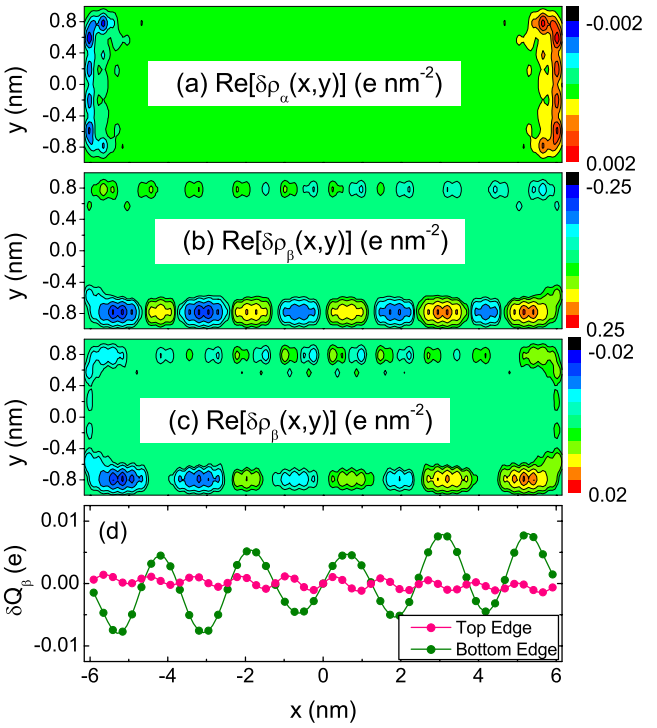

FIG. 4. (Color online) The dynamic charge response of the (8,99) ZGNR with strong substrate screening for (a) α and (b) β spins. The same response without any substrate screening for the β spin is shown in (c) and is an order-of-magnitude smaller. (d) shows the dynamic charge responses of β spin in (b) at the top and bottom edges of the (8,99) ZGNR. The dc electric field is $E_y^{\mathrm{dc}}=1.745$ V/nm, and the electric component of the EM wave is $E_x^{\mathrm{ac}}=0.01$ V/nm at $\omega=16$ GHz frequency.

tude of $E_x^{\mathrm{ac}}=0.01$ V/nm, which is within the linear-response regime. One can envision either a purely electric ac field or a photon field at the same frequency; the dipole approximation applies and the magnetic field is negligible.

The dynamic charge response function (δQ_σ) to the EM field is computed using the linear-response theory developed previously.[14] The results are plotted in Fig. 4. In order to show the charge response more vividly, we smooth the discrete site charges $\delta Q_\sigma(i)$ using a Gaussian function to obtain a spatial charge density,

$$\delta\rho_\sigma(\mathbf{r}) = \frac{4}{\pi a^2}\sum_i \exp\left(-\frac{4|\mathbf{r}-\mathbf{r}_i|^2}{a^2}\right)\delta Q_\sigma(i), \qquad (3)$$

where a is the lattice constant of graphene. We first examine the effect of substrate screening.[15] In Fig. 4 we compare the dynamic charge response of the (8,99) ZGNR with and without the substrate screening. In panels of Figs. 4(a) and 4(b), we assume a very strong screening from a substrate whose dielectric constant is essentially infinity. The strong screening induces the electrons in the ZGNR to behave as if they are essentially noninteracting, whereby the charge response is given directly by the linear-response susceptibility.[14] Compare this result with panel of Fig. 4(c), where no substrate screening is included and the dynamic charge response is one order-of-magnitude smaller. Note that the substrate screening does not affect the exchange interaction between electrons inside the GNR; thus it has no effect on the exchange coupling parameter J_{ij}. From this point on, we will focus only in the case with a strong substrate screening.

Comparing panels of Figs. 4(a) and 4(b), we see that the spin waves for the α spin are much weaker than for the β spin. The reason is that both the HOMO and the LUMO are β-spin states while all the α-spin states are farther away from the Fermi energy, whereby their response to the EM field is weaker. Because of this asymmetry in the response between the two spins, the net charge response is spin polarized whereby the standing waves are standing spin waves. Shown in Fig. 4(b) the standing spin waves are localized at the two zigzag edges.

The charge and the spin waves are from the cross terms between the HOMO and the LUMO wave functions which are mixed by the EM field. The wave vectors of the spin waves are simply the sum of the wave vectors of the HOMO and LUMO wave functions. Thus for the top edge we should expect $2k_v$. Because k_v is very close to the Brillouin-zone boundary, we should see $2\pi/a-2k_v$, or a wavelength of $5a$, in the actual spin wave. Similarly, for the bottom edge, we should see a wave vector $2\pi/a-k_v-k_c$, or a wavelength of $10a$. Thus, the unusual LUMO wave function that exhibits two different periods is predicted to give spin waves with different periods along each edge. Figure 4(d) shows the variation in the charge response δQ_β along the two edges, confirming the prediction of the two periods. The very long periods ($5a$ and $10a$) of these waves in graphene, compared to the Friedel oscillations which usually have periods comparable to lattice constants, makes graphene an excellent candidate for detecting and exploiting this effect.

Finally, we show in Fig. 5 that the resonance frequency of the standing spin waves can be tuned with the transverse dc

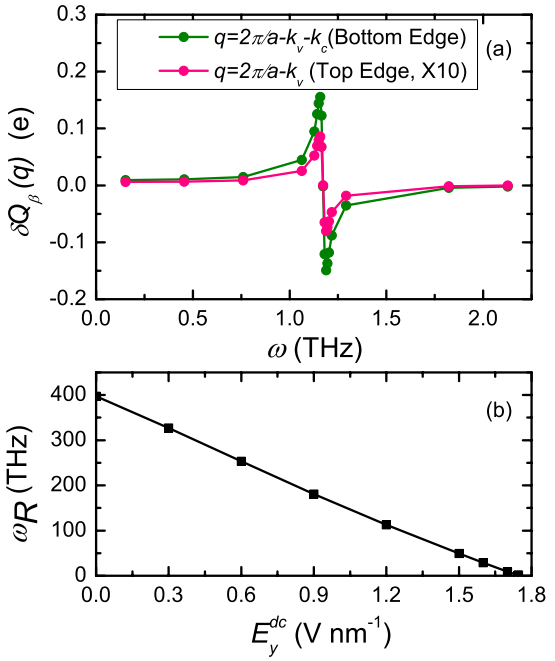

FIG. 5. (Color online) (a) The $q=2\pi/a-2k_v$ (top edge) and $q=2\pi/a-k_v-k_c$ (bottom edge) components of the Fourier transform of the standing spin waves as a function of the driving frequency with the transverse dc electric field $E_y^{\mathrm{dc}}=1.745$ V/nm; (b) The resonance frequency as a function of the transverse dc electric field.

electric field. When the frequency of the EM wave is varied, the amplitudes of the standing spin waves exhibit resonances as a function of the frequency. In order to show the resonances, we calculate the $q=2\pi/a-2k_v$ (top edge) and $q=2\pi/a-k_v-k_c$ (bottom edge) components of the Fourier transform $\delta Q_\beta(q)$ of the standing spin waves. Figure 5(a) shows the resonances of the standing spin waves at both edges under a transverse dc electric field $E_y^{\mathrm{dc}}=1.745$ V/nm. By varying the transverse dc electric field, one can tune the resonance frequency (ω_R). Figure 5(b) shows the resonance frequency as a function of the transverse dc electric field. This resonance frequency corresponds to the energy difference between the HOMO and the LUMO. The fact that this resonance can be tuned by an external dc voltage provides an additional controlling lever for potential applications.

In summary, the unique electronic structure of ZGNRs enables the excitation of resonant edge standing spin waves by electromagnetic radiation in the THz regime. The THz regime lies between traditional radio and light waves and has presented unique challenges. In recent years it has been possible to produce devices that emit and detect THz waves. Manipulation of THz radiation and the design of THz devices is a current frontier with promise for cutting-edge applications in communications, security, imaging, and medical applications.[10] Graphene nanoribbons provide a test bed for THz "optospintronics."

This research was conducted at the CNMS sponsored at ORNL by the Division of Scientific User Facilities, U.S. DOE. The work was further supported by the DOE Grant No. FDEFG0203ER46096, and by the McMinn Endowment at Vanderbilt University.

[1] H. Hiura, Appl. Surf. Sci. **222**, 374 (2004).
[2] K. S. Novoselov, A. K. Geim, S. V. Morozov, D. Jiang, M. I. Katsnelson, I. V. Grigorieva, S. V. Dubonos, and A. A. Firsov, Nature (London) **438**, 197 (2005).
[3] C. Berger, Z. Song, X. Li, X. Wu, N. Brown, C. Naud, D. Mayou, T. Li, J. Hass, A. N. Marchenkov, E. H. Conrad, P. N. First, and W. A. de Heer, Science **312**, 1191 (2006).
[4] Y. W. Son, M. L. Cohen, and S. G. Louie, Nature (London) **444**, 347 (2006).
[5] N. D. Lang and W. Kohn, Phys. Rev. B **1**, 4555 (1970).
[6] V. T. Renard, O. A. Tkachenko, V. A. Tkachenko, T. Ota, N. Kumada, J.-C. Portal, and Y. Hirayama, Phys. Rev. Lett. **100**, 186801 (2008).
[7] H. Lee, Y. W. Son, N. Park, S. Han, and J. Yu, Phys. Rev. B **72**, 174431 (2005).
[8] L. Pisani, J. A. Chan, B. Montanari, and N. M. Harrison, Phys. Rev. B **75**, 064418 (2007).
[9] O. V. Yazyev and M. I. Katsnelson, Phys. Rev. Lett. **100**, 047209 (2008).
[10] H.-T. Chen, W. J. Padilla, J. M. O. Zide, A. C. Gossard, A. J. Taylor, and R. D. Averitt, Nature (London) **444**, 597 (2006).
[11] L. Yang, M. L. Cohen, and S. G. Louie, Nano Lett. **7**, 3112 (2007).
[12] V. M. Pereira, F. Guinea, J. M. B. Lopes dos Santos, N. M. R. Peres, and A. H. Castro Neto, Phys. Rev. Lett. **96**, 036801 (2006).
[13] P. Koskinen, S. Malola, and H. Häkkinen, Phys. Rev. Lett. **101**, 115502 (2008).
[14] J. Q. Lu, X.-G. Zhang, and S. T. Pantelides, Phys. Rev. Lett. **99**, 226804 (2007).
[15] J. Lee and H. N. Spector, J. Appl. Phys. **57**, 366 (1985).